Field-induced magnetic reorientation and effective anisotropy of a ferromagnetic monolayer within spin wave theory

P. Fröbrich[1,2,a], P.J. Jensen[1,2], and P.J. Kuntz[1]

[1] Hahn-Meitner-Institut Berlin, Glienicker Straße 100, 14109 Berlin, Germany
[2] also Institut für Theoretische Physik, Freie Universität Berlin, Arnimallee 14, 14195 Berlin, Germany

Abstract. The reorientation of the magnetization of a ferromagnetic monolayer is calculated with the help of many-body Green's function theory. This allows, in contrast to other spin wave theories, a satisfactory calculation of magnetic properties over the entire temperature range of interest since interactions between spin waves are taken into account. A Heisenberg Hamiltonian plus a second-order uniaxial single-ion anisotropy and an external magnetic field is treated by the Tyablikov (Random Phase Approximation: RPA) decoupling of the exchange interaction term and the Anderson-Callen decoupling of the anisotropy term. The orientation of the magnetization is determined by the spin components $\langle S^\alpha \rangle$ ($\alpha = x, y, z$), which are calculated with the help of the spectral theorem. The knowledge of the orientation angle Θ_0 allows a non-perturbative determination of the temperature dependence of the effective second-order anisotropy coefficient. Results for the Green's function theory are compared with those obtained with mean-field theory (MFT). We find significant differences between these approaches.

PACS. 75.10.Jm Quantized spin models – 75.30.Ds Spin waves – 75.70.Ak Magnetic properties of monolayers and thin films

1 Introduction

Experimental and theoretical investigations of the magnetic properties of ultrathin ferromagnetic films are a topic of intense current interest [1]. In particular, the temperature dependent (effective) magnetic anisotropy and the resulting direction of the magnetization have been determined for a variety of thin film systems [2]. The different temperature and thickness dependence of the various anisotropy contributions may result in a reorientation of the magnetization as function of temperature and/or film thickness. In addition, a magnetic reorientation can be induced by applying a magnetic field [3,4], which is one of the experimental methods for measuring the magnetic anisotropies. In order to determine the different contributions to the magnetic anisotropy separately, their dependence on the temperature, on the film thickness, and on the magnetic field has to be known.

By use of *ab-initio* methods, the magnetic anisotropy of thin films has been calculated as the total energy difference between different directions of the magnetization [5]. Until now this has been done only for $T = 0$, whereas measurements are always performed at finite temperatures. Thus, the knowledge of the temperature dependence of the anisotropies is also required in order to allow a comparison of experimental and theoretical results.

This knowledge is gained mainly within the framework of a Heisenberg model for localized spins, which, however, seems to yield satisfactory results also for the important case of itinerant magnets such as Fe, Co, and Ni. Usually mean-field theory (MFT) is applied to calculate the magnetization, accompanied either by diagonalization of a single-particle Hamiltonian [6], or by a thermodynamic perturbation theory for the anisotropy terms [7]. In principle, MFT is not applicable to two-dimensional (2D) magnetic systems. In such systems, thermodynamic correlations, which are neglected by MFT, have a decisive influence on the magnetic properties. In particular, the long-range magnetic fluctuations destroy the remanent magnetization of an *isotropic* 2D Heisenberg model at finite temperatures (Mermin-Wagner theorem [8]). However, even small anisotropic contributions, which are always present in real magnetic systems, induce a magnetically ordered state in thin films with a critical temperature of the order of the exchange coupling [9]. This is the reason why results obtained from MFT are expected to be *qualitatively* correct also for 2D Heisenberg magnets. Furthermore, it is known that applied magnetic fields have a much larger impact on the magnetic properties of 2D than of three-dimensional (3D) systems [10]. Therefore, measured magnetic quantities such as the effective anisotropy may in principle depend on the experimental situation, *e.g.* whether a magnetic field is present or not. The MFT

[a] e-mail: `froebrich@hmi.de`

method poorly reproduces this sensitive field dependence of 2D systems, thus necessitating an improved theoretical description.

Long-range magnetic fluctuations can be treated by spin wave theories. To our knowledge, the calculation of a field-induced magnetic reorientation with such an approach has been performed only by Erickson and Mills [11], who consider an exchange coupling, a uniaxial lattice anisotropy, and the magnetic dipole coupling. They have transformed the spin operators into Bose operators (Holstein-Primakoff transformation [12]), which are treated only in lowest order. Thus the validity of this linearized spin wave theory is limited to low temperatures. The authors obtained a strong increase of the transverse fluctuations near the reorientation transition, where the direction of magnetization turns into the field direction. However, as remarked by the authors, the method should break down in this region.

In a previous paper [13], we demonstrated with the help of a many-body Green's function theory that the Tyablikov (or RPA) decoupling [14] of the higher-order Green's functions provides a significantly improved description of the magnetization over MFT. We showed this by comparing RPA and MFT results with the exact solution of a Heisenberg spin pair, and with the "exact" quantum Monte Carlo result [15] of a Heisenberg monolayer with spin $S = 1/2$. Also the temperature dependence of the second- and fourth-order effective anisotropy coefficients was calculated by a thermodynamic perturbation theory, expecting that RPA gives an improved description also for the effective anisotropy coefficients. As results we found that their temperature dependence looks different, particularly at low temperatures, and that their dependence on the magnitude of the spin is much weaker in RPA than in MFT [13]. Such a perturbative approach makes sense only if the magnetic field is stronger than the anisotropy.

In the present work, we investigate also in the framework of many-body Green's function theory the orientation of a ferromagnetic monolayer at finite temperatures, the field-induced magnetic reorientation, and the effective (temperature-dependent) anisotropy. Encouraged by the fact that RPA yields a good approximation to the magnetization, we expect that the RPA results of the present paper also represent more satisfactory estimates for the above mentioned magnetic properties than the results of MFT. Added to the Heisenberg Hamiltonian is the second-order single-ion anisotropy favoring a perpendicular magnetization, and an external magnetic field perpendicular to this uniaxial lattice anisotropy, causing a magnetic reorientation with an increasing field strength. Since we are mainly interested in the action of the second order *single-ion* anisotropy and its temperature dependence, we omit here the magnetic dipole coupling. For a ferromagnetic monolayer the dipole coupling competing with the out-of-plane second order single-ion anisotropy will induce a reorientation as a function of the temperature only in a narrow parameter range (for the strengths of the dipole coupling and the anisotropy) and therefore a reorientation

is quite improbable in general, see *e.g.* [16]. The magnetization of a monolayer will in most cases stay either in-plane or out-of plane. This is the reason why we study the reorientation induced by an external magnetic field. For several layers, on the other hand, the dipole coupling will play a more important role. A magnetic reorientation as function of film thickness and/or temperature can be expected, when the film surface and film interior anisotropic contributions compete with each other and exhibit different temperature dependences.

We apply the RPA method for decoupling the Green's functions coming from the exchange coupling terms thus approximately taking into account interactions between magnons, whereas we make use of the Anderson-Callen decoupling [17] for the corresponding anisotropy terms. The magnetization axis will be tilted with respect to the easy axis by the magnetic field; this procedure resembles the experimental situation [2,3]. We do not rotate the local spin quantization axis but calculate the magnetization from the expectation values of the spin components $\langle S^\alpha \rangle$. This gives the equilibrium orientation angle directly. Knowledge of the orientation angle allows a calculation of the temperature dependent (effective) anisotropy coefficient from the condition that the free energy be a minimum. This is a non-perturbative approach because the quantities entering in the final expression are calculated from the *full* Hamiltonian. This is an improvement over the previously [13] used thermodynamic perturbation theory, where the anisotropy term is treated as a small perturbation. We compare the effective anisotropy obtained from the non-perturbative approach with that from the thermodynamic perturbation theory and, in many places throughout the paper, we compare the results obtained from the Green's function theory with those from MFT.

2 The Green's function formalism

Our aim is to determine the orientation angle $\Theta_0(T)$ of the magnetization of a single (001)-layer as a function of the temperature T from the expectation values $\langle S^\alpha \rangle$ ($\alpha = x, y, z$) of the components of the magnetization. For this purpose a Heisenberg Hamiltonian is used [6,7] consisting of the isotropic exchange interaction J between nearest neighbour lattice sites, a second-order single-ion anisotropy parameter $K_2 = K_2(T = 0)$ at zero temperature, and an external magnetic field, $\mathbf{B} = (B^x, B^y, B^z)$

$$
\begin{aligned}
\mathcal{H} = &-\frac{J}{2} \sum_{kl} \mathbf{S}_k \mathbf{S}_l - K_2 \sum_k (S_k^z)^2 - \sum_k \mathbf{B}\,\mathbf{S}_k \\
= &-\frac{J}{2} \sum_{kl} (S_k^- S_l^+ + S_k^z S_l^z) - K_2 \sum_k (S_k^z)^2 \\
&- \sum_k \left(\frac{1}{2} B^- S_k^+ + \frac{1}{2} B^+ S_k^- + B^z S_k^z\right),
\end{aligned}
\tag{1}
$$

where the notation $S_i^\pm = S_i^x \pm \mathrm{i} S_i^y$ and $B^\pm = B^x \pm \mathrm{i} B^y$ is introduced.

In order to treat the problem, one needs the following Green's functions:

$$G_{ij(\eta)}^{\alpha,mn} = \langle\langle S_i^\alpha ; (S_j^z)^m (S_j^-)^n \rangle\rangle ; \quad \alpha = +, -, z , \qquad (2)$$

where $\eta = \pm 1$ refer to the commutator ($\eta = -1$) or anti-commutator ($\eta = 1$) Green's functions, respectively, $n \geq 1$ and $m \geq 0$ are positive integers, i and j denote lattice sites.

The $G_{ij(\eta)}^{\alpha,mn}$ are determined from the equations of motion in the spectral representation

$$\omega G_{ij(\eta)}^{\alpha,mn}(\omega) = A_{ij(\eta)}^{\alpha,mn} + \langle\langle [S_i^\alpha, \mathcal{H}]_{-1} ; (S_j^z)^m (S_j^-)^n \rangle\rangle_\omega , \tag{3}$$

with the inhomogeneities

$$A_{ij(\eta)}^{\alpha,mn} = \langle [S_i^\alpha, (S_j^z)^m (S_j^-)^n]_\eta \rangle$$
$$= \langle S_i^\alpha (S_j^z)^m (S_j^-)^n + \eta (S_j^z)^m (S_j^-)^n S_i^\alpha \rangle , \qquad (4)$$

where $\langle...\rangle = \mathrm{Tr}(...\mathrm{e}^{-\beta\mathcal{H}})$ with $\beta = 1/k_B T$ and k_B Boltzmann's constant.

Knowledge of the Green's functions allows the determination of the respective correlation functions by the spectral theorem [14]

$$C_{ij}^{\alpha mn} = \langle (S_j^z)^m (S_j^-)^n S_i^\alpha \rangle$$
$$= \frac{\mathrm{i}}{2\pi} \lim_{\delta \to 0} \int_{-\infty}^{\infty} \frac{\mathrm{d}\omega}{\mathrm{e}^{\beta\omega} + \eta} \left[G_{ij(\eta)}^{\alpha,mn}(\omega + \mathrm{i}\delta) - G_{ij(\eta)}^{\alpha,mn}(\omega - \mathrm{i}\delta) \right]. \tag{5}$$

Calculation of the commutators $[S_i^\alpha, H]_{-1}$ yields the following set of equations of motion for the Green's functions

$$\omega G_{ij(\eta)}^{\pm,mn} = A_{ij(\eta)}^{\pm,mn} \mp J \sum_k \left(\langle\langle S_i^z S_k^\pm ; (S_j^z)^m (S_j^-)^n \rangle\rangle \right.$$

$$- \langle\langle S_k^z S_i^\pm ; (S_j^z)^m (S_j^-)^n \rangle\rangle)$$

$$\pm K_2 \langle\langle (S_i^\pm S_i^z + S_i^z S_i^\pm) ; (S_j^z)^m (S_j^-)^n \rangle\rangle$$

$$\mp B^\pm G_{ij(\eta)}^{z,mn} \pm B^z G_{ij(\eta)}^{\pm,mn}$$

$$\omega G_{ij(\eta)}^{z,mn} = A_{ij(\eta)}^{z,mn} + \frac{J}{2} \sum_k \langle\langle (S_i^- S_k^+ - S_k^- S_i^+) ;$$

$$(S_j^z)^m (S_j^-)^n \rangle\rangle$$

$$- \frac{1}{2} B^- G_{ij(\eta)}^{+,mn} + \frac{1}{2} B^+ G_{ij(\eta)}^{-,mn}. \tag{6}$$

The higher-order Green's functions occurring on the right-hand sides have to be decoupled in order to obtain a closed set of equations. For the exchange coupling terms we apply a generalized Tyablikov- (or RPA-) [14,20] decoupling, allowing also for a finite value of the x, y- (or $\pm$-) components of the magnetization ($\alpha, \beta = +, -, z; i \neq k$)

$$\langle\langle S_i^\alpha S_k^\beta ; (S_j^z)^m (S_j^-)^n \rangle\rangle \simeq \langle S_i^\alpha \rangle G_{kj}^{\beta,mn} + \langle S_k^\beta \rangle G_{ij}^{\alpha,mn} . \tag{7}$$

The terms resulting from the single-ion anisotropy ($i = k$) have to be decoupled differently. A RPA-decoupling, as

was proposed by Narath [21], is reasonable for an exchange anisotropy ($\propto S_i^z S_k^z$). It yields for the single-ion anisotropy unphysical results, for instance for $S = 1/2$ the respective terms do not vanish. Instead, an ansatz of the following form is introduced [22]

$$\langle\langle S_i^\pm S_i^z + S_i^z S_i^\pm ; (S_j^z)^m (S_j^-)^n \rangle\rangle \simeq \Phi_i^{\pm,mn} G_{ij}^{\pm,mn}, \tag{8}$$

where the functions $\Phi_i^{\pm,mn}$ have to be determined. This type of decoupling is valid for anisotropies which are small compared to the exchange interaction. In Appendix A, we have investigated various decoupling schemes for the single-ion anisotropy proposed in the literature. In the appendix, we give arguments for our preferring the Anderson-Callen decoupling for the present calculations, yielding the decoupling function for $n = 1$

$$\Phi \equiv \Phi_i^{\pm,m1} \simeq 2\langle S_i^z \rangle \left(1 - \frac{1}{2S^2} [S(S+1) - \langle S_i^z S_i^z \rangle] \right) . \tag{9}$$

We now apply the Tyablikov decoupling to the exchange interaction term and the Anderson-Callen decoupling to the single-ion anisotropy term in equations (6). Performing in addition a 2D-Fourier transformation to momentum space, with $\mathbf{k} = (k_x, k_y, 0)$ being the in-plane wave vector, yields the following set of equations of motion

$$\begin{pmatrix} \omega - \tilde{H}^z & 0 & H^+ \\ 0 & \omega + \tilde{H}^z & -H^- \\ \frac{1}{2}H^- & -\frac{1}{2}H^+ & \omega \end{pmatrix} \begin{pmatrix} G_\eta^{+,mn}(\mathbf{k}, \omega) \\ G_\eta^{-,mn}(\mathbf{k}, \omega) \\ G_\eta^{z,mn}(\mathbf{k}, \omega) \end{pmatrix}$$
$$= \begin{pmatrix} A_\eta^{+,mn} \\ A_\eta^{-,mn} \\ A_\eta^{z,mn} \end{pmatrix}, \tag{10}$$

with the abbreviations

$$H^\alpha = B^\alpha + \langle S^\alpha \rangle J(q - \gamma_\mathbf{k}), \qquad \alpha = +, -, z$$
$$\tilde{H}^z = H^z + K_2 \Phi = Z + \langle S^z \rangle J(q - \gamma_\mathbf{k})$$
$$Z = B^z + K_2 \Phi. \tag{11}$$

For a square lattice, one obtains $\gamma_\mathbf{k} = 2(\cos k_x + \cos k_y)$, and $q = 4$ is the number of nearest neighbours. Note that $A_\eta^{\alpha,mn} = A_\eta^{\alpha,mn}(\mathbf{k})$ depends on the wave vector $\mathbf{k}$ for $\eta = 1$ but not for $\eta = -1$.

The determinant of the matrix in equation (10) is given by

$$\Delta(\omega, \mathbf{k}) = \omega(\omega - E_\mathbf{k})(\omega + E_\mathbf{k}),$$
$$\text{with} \quad E_\mathbf{k} = \sqrt{H^+ H^- + \tilde{H}^z \tilde{H}^z}, \tag{12}$$

which is the magnon dispersion relation. Hence, the eigenvalues are

$$\omega_1 = 0 , \quad \omega_{2,3} = \pm E_\mathbf{k}. \tag{13}$$

The Green's functions are given by

$$G_\eta^{\alpha,mn}(\omega, \mathbf{k}) = \frac{\Delta_\eta^{\alpha,mn}(\omega, \mathbf{k})}{\Delta(\omega, \mathbf{k})}, \qquad \alpha = +, -, z, \tag{14}$$

where $\Delta_\eta^{\alpha,mn}$ is the determinant where column α of Δ is replaced by the right-hand side of equation (10). One obtains, for example

$$\Delta_\eta^{z,mn}(\omega,\mathbf{k}) = A_\eta^{z,mn}\left(\omega^2 - (\tilde{H}^z)^2\right) - \frac{1}{2}A_\eta^{+,mn}H^-(\omega + \tilde{H}^z)$$
$$+ \frac{1}{2}A_\eta^{-,mn}H^+(\omega - \tilde{H}^z). \tag{15}$$

Now we use the fact that the *commutator* Green's functions must be regular for $\omega \to 0$, *e.g.* [14],

$$\lim_{\omega\to 0}\omega G_{-1}^{\alpha,mn}(\omega,\mathbf{k}) = 0. \tag{16}$$

Thus $\Delta_{-1}^{\alpha,mn}(0,\mathbf{k}) = 0$. Since one of the eigenvalues vanishes, see equation (13), we obtain from equation (15) for $\tilde{H}^z \neq 0$

$$H^-A_{-1}^{+,mn} + H^+A_{-1}^{-,mn} + 2\tilde{H}^zA_{-1}^{z,mn} = 0. \tag{17}$$

Evaluating this expression for $m = 0$ and $n = 1$ we find together with the definitions in equation (11)

$$\frac{H^\pm}{\tilde{H}^z} = \frac{B^\pm}{B^z + K_2\Phi} = \frac{B^\pm}{Z}. \tag{18}$$

Putting this into equation (17) we have

$$-2Z A_{-1}^{z,mn} = A_{-1}^{+,mn}B^- + A_{-1}^{-,mn}B^+. \tag{19}$$

Equations (17) and (19) are important relations between correlation functions which we call the *regularity conditions.* We note that the same relations are obtained for all three $\alpha = +,-,z$. With $m = 0$ and $n = 1$ we obtain a relation between $\langle S^\pm\rangle$ and $\langle S^z\rangle$

$$\langle S^\pm\rangle = \frac{B^\pm}{Z}\langle S^z\rangle$$
$$= \frac{B^\pm\langle S^z\rangle}{B^z + 2K_2\langle S^z\rangle\left(1 - [S(S+1) - \langle S^zS^z\rangle]/2S^2\right)}. \tag{20}$$

This means that the knowledge of $\langle S^z\rangle$ and $\langle S^zS^z\rangle$ also determines the expectation value of the spin components $\langle S^x\rangle$ and $\langle S^y\rangle$. Other useful relations obtained from equation (19) are given in Appendix B.

It remains to establish equations which determine the moments $\langle (S^z)^m\rangle$. For this purpose we consider for example the following commutator Green's function

$$G_{-1}^{z,mn}(\omega,\mathbf{k}) = \frac{\Delta_{-1}^{z,mn}(\omega,\mathbf{k})}{\Delta(\omega,\mathbf{k})}$$
$$= \frac{1}{\omega(\omega - E_\mathbf{k})(\omega + E_\mathbf{k})}\left(-A_{-1}^{+,mn}\frac{1}{2}H^-\omega\right.$$
$$\left. + A_{-1}^{-,mn}\frac{1}{2}H^+\omega + A_{-1}^{z,mn}\omega^2\right), \tag{21}$$

where the regularity condition has been taken into account.

In order to calculate correlation functions in the case of a vanishing eigenvalue one also needs the respective *anti-commutator* Green's function $G_{+1}^{z,mn}$, since in this case the correct form of the spectral theorem reads, *e.g.* [14]

$$C_\mathbf{k}^{zmn} = \frac{\mathrm{i}}{2\pi}\lim_{\delta\to 0}\int_{-\infty}^\infty \frac{\mathrm{d}\omega}{\mathrm{e}^{\beta\omega} - 1}\left[G_{-1}^{z,mn}(\omega + \mathrm{i}\delta,\mathbf{k})\right.$$
$$\left. - G_{-1}^{z,mn}(\omega - \mathrm{i}\delta,\mathbf{k})\right] + D_\mathbf{k}^{z,mn}, \tag{22}$$

where

$$D_\mathbf{k}^{z,mn} = \lim_{\omega\to 0}\frac{\omega}{2}G_{+1}^{z,mn}(\omega,\mathbf{k}). \tag{23}$$

Using

$$G_{+1}^{z,mn}(\omega,\mathbf{k}) = \frac{\Delta_{+1}^{z,mn}(\omega,\mathbf{k})}{\Delta(\omega,\mathbf{k})} = \frac{1}{\omega(\omega - E_\mathbf{k})(\omega + E_\mathbf{k})}$$
$$\times \left(-A_{+1}^{+,mn}\frac{1}{2}H^-(\omega + \tilde{H}^z) + A_{+1}^{-,mn}\frac{1}{2}H^+(\omega - \tilde{H}^z)\right.$$
$$\left. + A_{+1}^{z,mn}\left(\omega^2 - (\tilde{H}^z)^2\right)\right), \tag{24}$$

and the relation between anti-commutator and commutator correlation functions

$$A_{+1}^{\alpha,mn}(\mathbf{k}) = A_{-1}^{\alpha,mn} + 2C_\mathbf{k}^{\alpha mn}, \tag{25}$$

we find together with the regularity condition

$$D_\mathbf{k}^{z,mn} = \frac{1}{2E_\mathbf{k}^2}\left(C_\mathbf{k}^{+mn}H^-\tilde{H}^z\right.$$
$$\left. + C_\mathbf{k}^{-mn}H^+\tilde{H}^z + 2C_\mathbf{k}^{zmn}(\tilde{H}^z)^2\right). \tag{26}$$

Finally, we obtain from equation (22) together with equations (21) and (26)

$$2H^+H^-C_\mathbf{k}^{zmn} - H^-\tilde{H}^zC_\mathbf{k}^{+mn} - H^+\tilde{H}^zC_\mathbf{k}^{-mn} =$$
$$A_{-1}^{+,mn}\frac{1}{2}E_\mathbf{k}H^-\left[\frac{E_\mathbf{k}}{\tilde{H}^z} - \coth(\beta E_\mathbf{k}/2)\right]$$
$$+ A_{-1}^{-,mn}\frac{1}{2}E_\mathbf{k}H^+\left[\frac{E_\mathbf{k}}{\tilde{H}^z} + \coth(\beta E_\mathbf{k}/2)\right]. \tag{27}$$

From these relations and the regularity conditions, equation (19), one obtains all necessary expectation values.

In the following we restrict ourselves to an external magnetic field $\mathbf{B}$ confined to the xz-plane. Because of the azimuthal symmetry in the case of an uniaxial anisotropy it is sufficient to deal with the z- and x-components of

the magnetization ($\langle S^y \rangle = 0$ for $B^y = 0$). From these values the magnitude and the equilibrium polar angle of the magnetization are determined:

$$M^2(T) = \langle S^x \rangle^2 + \langle S^z \rangle^2 \,,$$
$$\Theta_0(T) = \arctan \frac{\langle S^x \rangle}{\langle S^z \rangle} = \arctan \frac{B^x}{B^z + K_2 \Phi} \,. \quad (28)$$

The knowledge of $M(T)$ and Θ_0 enables a non-perturbative determination of the temperature dependence of the anisotropy coefficient. The anisotropic part of the free energy is usually written as a power series of the direction cosines of the magnetization. Its precise form is written in accordance with the symmetry of the system and usually converges. This series need not only be valid for small fields and anisotropies as compared to the exchange coupling. It can even be considered as a definition of the effective (temperature-dependent) anisotropy coefficients. It is such an expression from which experimentalists determine the effective anisotropies. The corresponding part of the free energy in the presence of the lowest order term, the second-order uniaxial anisotropy $K_2(T)$, and the Zeeman term has the form

$$F(T, \Theta) = F_0(T) - K_2(T) \cos^2 \Theta - \mathbf{B} \cdot \mathbf{M(T)} \,. \quad (29)$$

This corresponds to the physical situation where the higher order anisotropies can be neglected. We only treat this case in the present paper. $K_2(T)$ is then determined from the condition that the free energy has a minimum at the equilibrium angle Θ_0:

$$\frac{\partial F(\Theta)}{\partial \Theta}(\Theta_0) = 0 = 2 K_2(T) \cos \Theta_0 \sin \Theta_0$$
$$- B^x M(T) \cos \Theta_0 + B^z M(T) \sin \Theta_0 \,. \quad (30)$$

Solving with respect to $K_2(T)$ we find

$$K_2(T) = \frac{M(T)(B^x \cos \Theta_0 - B^z \sin \Theta_0)}{2 \cos \Theta_0 \sin \Theta_0} \,. \quad (31)$$

Note that the effective anisotropy can be considered as an intrinsic property of the layer itself only if $K_2(T)$ as obtained by equation (31) is practically independent of the external magnetic field. We mention that the effective anisotropy at zero temperature $K_2(T=0)$ differs from the K_2 in the Hamiltonian by a spin-dependent normalization factor [6,18]. By expanding equations (9), (28) and (31) for small T and Θ_0 one finds $K_2(T=0) = K_2 S(S-1/2)$. The results shown in Figures 3, 4, 6 are normalized with respect to this factor for $S=1$.

The procedure described above is non-perturbative in the sense that the quantities (the magnetization and the orientation angle) entering in equation (31) are calculated from the *full* Hamiltonian. This is in contrast to a thermodynamic perturbation theory in which the lattice anisotropy is used as a small perturbation. The Hamiltonian is split into two terms $\mathcal{H} = \mathcal{H}_0 - K_2 \sum_l (S_l^z)^2$, and

the effective anisotropy is calculated from moments of the unperturbed Hamiltonian $\mathcal{H}_0$ only, (see *e.g.* Ref. [13]).

In the present thermodynamic approach $K_2(T)$ depends on the temperature mainly through the magnetization, which itself is a function of the magnetic field. Thus at least a weak field dependence of the effective anisotropy is expected. There are other sources which might induce a temperature dependence. In reference [19] it has been shown within a tight-binding scheme that at a *constant* magnetization, the electronic entropy, the thermal lattice expansion, the population change of spin-orbit-splitted energy levels near the Fermi energy cause a decrease in the uniaxial anisotropy of a freestanding Fe monolayer at a temperature of about 1000 K. However, the magnetization and thus the resulting effective anisotropy will already have vanished below 500 K for this case. Therefore the decreasing magnetization is the main source for the temperature dependence of $K_2(T)$ in the temperature range we are looking at in the present paper.

In the following, we treat as an example $S = 1$, which is the lowest spin value with a nontrivial second-order anisotropy. For this case, the single-ion decoupling function reads $\Phi = \langle S^z \rangle \langle S^z S^z \rangle$, see equation (9). Then we obtain from equation (27) with $n = 1, m = 0$ and $n = 1, m = 1$, respectively, two coupled equations for $\langle S^z \rangle$ and $\langle S^z S^z \rangle$, after taking into account the regularity conditions of Appendix B for $S = 1$. The resulting equations are

$$\langle S^z S^z \rangle - \frac{2}{1 + (\frac{B^x}{Z})^2} + \frac{\langle S^z \rangle}{2} \frac{\left(2 - (\frac{B^x}{Z})^2\right)}{\sqrt{1 + (\frac{B^x}{Z})^2}} \phi(T) = 0, \quad (32)$$

$$\langle S^z \rangle \left(1 - (\frac{B^x}{Z})^2\right)\left(2 - (\frac{B^x}{Z})^2\right) + 2\langle S^z S^z \rangle \left(1 + (\frac{B^x}{Z})^2\right)$$
$$- 4 - \left[2(3\langle S^z S^z \rangle - 2)\left(1 - (\frac{B^x}{Z})^2\right)\right.$$
$$\left. - \langle S^z \rangle \left(2 - (\frac{B^x}{Z})^2\right)\right] \sqrt{1 + (\frac{B^x}{Z})^2} \, \phi(T) = 0, \quad (33)$$

with

$$\phi(T) = \frac{1}{\pi^2} \int_0^\pi \mathrm{d}k_x \int_0^\pi \mathrm{d}k_y \coth\left(\beta E_\mathbf{k}/2\right). \quad (34)$$

These equations have to be solved numerically in order to obtain $\langle S^z \rangle$ and $\langle S^z S^z \rangle$. Together with equation (20) these determine the magnitude $M(T)$ and the orientation angle Θ_0 of the magnetization, *cf.* equations (28).

In the next section we compare the RPA method with a (Bragg-Williams) mean field approximation for the exchange coupling term for a quantum-mechanical spin $S = 1$. The resulting expectation values are obtained by diagonalizing the corresponding dynamical matrix consisting of the molecular field, the external magnetic field and the single-ion anisotropy. For details see reference [6].
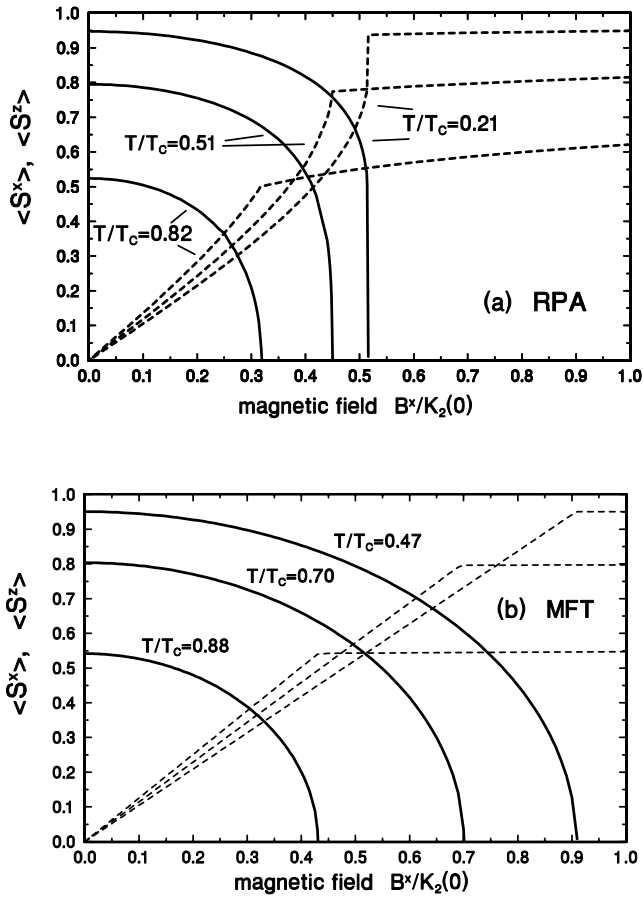
Fig. 1. Components of the magnetization $\langle S^z \rangle$ (solid lines) and $\langle S^x \rangle$ (dashed lines) for different reduced temperatures T/T_C as functions of the external magnetic field in x-direction, $B^x/K_2(0)$, which is normalized to the anisotropy coefficient at temperature $T = 0$. Results of RPA (a) and MFT (b) calculations are compared. The Curie temperatures are $T_C^{\mathrm{RPA}}/J = 0.989$ within RPA, and $T_C^{\mathrm{MFT}}/J = 2.667$ within MFT, using $J/K_2(0) = 100$. The reduced temperatures in (a) and (b) are chosen in such a way that the magnetization $\langle S^z \rangle$ are approximately the same in RPA and MFT at $B^x = 0$.

Fig. 2. The orientation angle Θ_0 of the magnetization is shown as a function of $B^x/K_2(0)$ for the same reduced temperatures as in Figure 1. RPA results (a) are compared with MFT results (b).

3 Results

In this section, we display results of our calculations for a Heisenberg Hamiltonian plus second-order uniaxial single-ion anisotropy for a square monolayer with spin $S = 1$. If not stated otherwise, the interactions will be normalized to the single-ion anisotropy coefficient at zero temperature $K_2 = K_2(T = 0) > 0$. We use for the exchange coupling $J/K_2(0) = 100$. With zero magnetic field and these parameters, the RPA method predicts a Curie temperature $T_C^{\mathrm{RPA}}/J = 0.989$, *cf.* Appendix A. The mean-field theory yields with the same parameters a Curie temperature $T_C^{\mathrm{MFT}}/J = 2.667$, which is about a factor of three larger. The temperature at which the magnetization reaches the
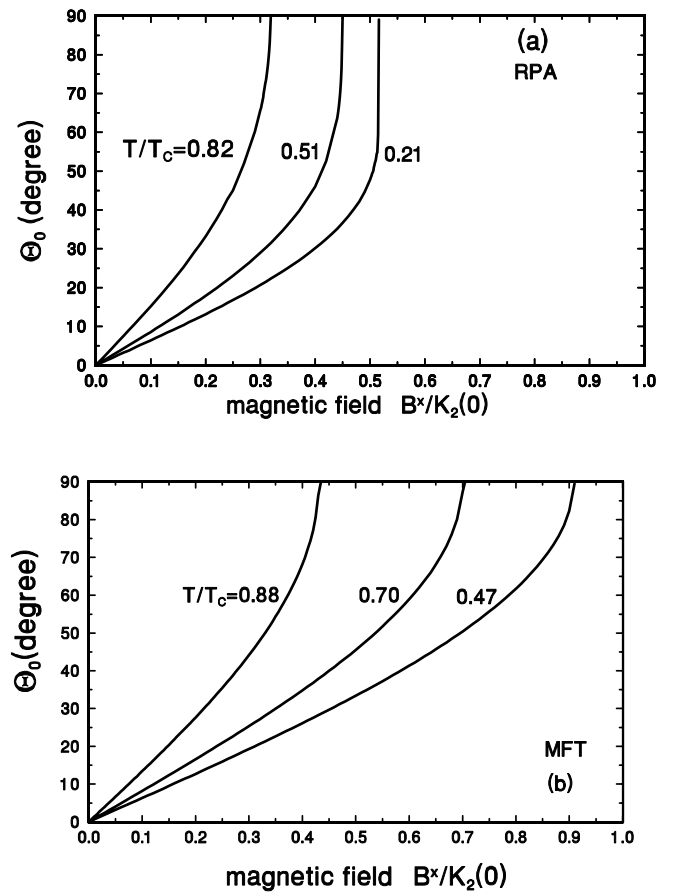
field direction ($\langle S^z \rangle \to 0$) is called the *reorientation temperature* T_R, and the corresponding magnetic field the *reorientation field* B_R^x.

In Figure 1a we show the results obtained from the RPA method for the components of the magnetization, $\langle S^z \rangle$ and $\langle S^x \rangle$, as functions of the external magnetic field $B^x/K_2(0)$ in x-direction ($B^y = B^z = 0$), for different reduced temperatures T/T_C. This field-induced magnetic reorientation is characterized by a decreasing $\langle S^z \rangle$ and an increasing $\langle S^x \rangle$. The magnetization reaches the in-plane direction ($\langle S^z \rangle = 0$) at a field strength B_R^x depending on the temperature. For the lowest temperature ($T/T_C = 0.21$), we observe a jump in the components of the magnetization at the corresponding reorientation field of about $B^x/K_2(0) \simeq 0.52$. This is probably caused by the particular kind of the single-ion anisotropy decoupling applied in our procedure. After complete reorientation $\langle S^x \rangle$ shows a nearly constant behaviour with increasing field. In Figure 1b we show the corresponding MFT results with the same parameters for J and $K_2(0)$. In order to
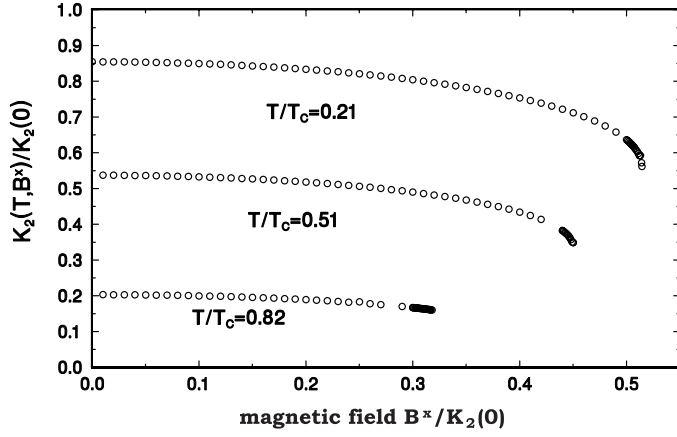
Fig. 3. Non-perturbative RPA-calculations for the effective single-ion anisotropy coefficient $K_2(T, B^x)$ normalized to $K_2(0)$ are shown as a function of the external magnetic field $B^x/K_2(0)$ for different reduced temperatures T/T_C.

Fig. 4. Effective anisotropy coefficient $K_2(T)/K_2(0) = 0.1$ and orientation angle $\Theta_0(T)$ are shown as functions of the reduced temperatures T/T_C. Large dots correspond to RPA, and small squares to MFT results.

compare the different shapes of the magnetization curves in RPA and MFT, we have chosen different reduced temperatures T/T_C^{MFT} for the MFT calculations in such a way that the relative magnetizations $\langle S^z \rangle$ at $B^x = 0$ are about the same in both cases. One observes that $\langle S^z \rangle$ decreases near B_R^x more rapidly within the RPA approach than within MFT. Also, whereas $\langle S^x \rangle$ as computed with MFT exhibits an almost linear behaviour as a function of $B^x/K_2(0)$, the corresponding RPA-dependence is clearly curved. The main difference is that the reorientation fields B_R^x are considerably smaller within the RPA approach for all temperatures investigated. This we attribute to the fact that a magnetic field has a stronger influence on 2D than on 3D systems. Note that the MFT results depend only on the coordination number and not on the spatial dimensionality, thus MFT handles a 2D system similar to a 3D one.

In Figure 2 we display the orientation angles $\Theta_0(T, B^x)$ corresponding to the situation of Figure 1 from a perpendicular ($\Theta_0 = 0°$) to an in-plane direction ($\Theta_0 = 90°$) of the monolayer magnetization.

The effective anisotropy coefficient, $K_2(T)$, is determined by equation (31), which we apply for $B^z = 0$. As mentioned before, this ansatz is physically meaningful only if the dependence of $K_2(T)$ on B^x is small. In Figure 3 the corresponding dependence is shown for different temperatures. For all temperatures we obtain only a weak dependence of $K_2(T)$ on $B^x/K_2(0)$ for small fields, which becomes stronger as the reorientation field strength B_R^x is approached. Therefore, we have used the small value $B^x/K_2(0) = 0.1$ to determine $K_2(T)$ as a function of the reduced temperature. In this case the reorientation temperature T_R is close to T_C. The resulting effective anisotropy $K_2(T)/K_2(0)$ and the corresponding orientation angle $\Theta_0(T)$ are shown in Figure 4. $K_2(T)$ as obtained from RPA is an almost straight line between $T = 0$ and $T = T_R \simeq T_C$. On the other hand, the corresponding
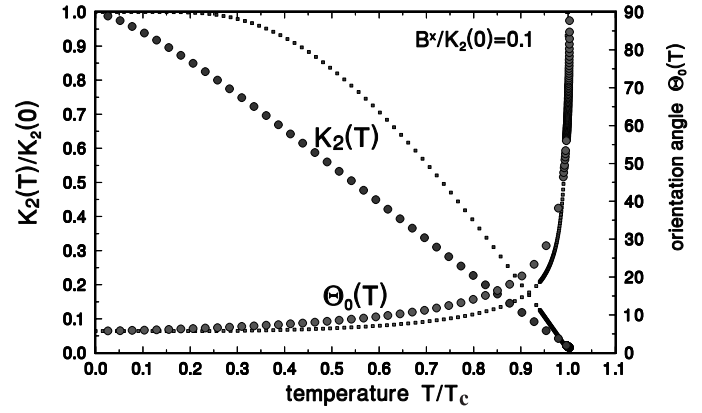
behaviour of $K_2(T)$ calculated by MFT is linear at elevated temperatures but shows an exponential behaviour when approaching $T = 0$. This has the consequence that for $S = 1$ the MFT approach yields a considerably smaller value of $K_2(0)$ than the RPA method, if observed values of $K_2(T)$ (measured *e.g.* at $T/T_C \sim 0.7$ [2]) are extrapolated to $T = 0$. Only at $T = 0$ are anisotropy constants from *ab-initio* calculations available which can then be compared with extrapolated measurements. Note that the range of the exponential behaviour of $K_2(T)$ when applying MFT [6,7] shrinks for large S or for classical spins.

We do not observe a large difference between RPA and MFT results for the orientation angle $\Theta_0(T)$ as a function of the reduced temperature T/T_C. Note, however, the different temperature scale. T_C as obtained from MFT is 2.7 times larger than the corresponding RPA result for the parameters under consideration.

In Figure 4 the reorientation temperature is close to the Curie temperature, since we have used a small field of $B^x/K_2(0) = 0.1$. When applying a larger field, for instance $B^x/K_2(0) = 0.4$, the reorientation takes place at lower temperatures. This is demonstrated in Figure 5a, which shows $\langle S^z \rangle$ and $\langle S^x \rangle$ as functions of the reduced temperature resulting from RPA calculations, yielding a reorientation temperature of about $T_R \simeq 0.65\,T_C$. The corresponding magnitude of the magnetization $M(T) = \sqrt{\langle S^x \rangle^2 + \langle S^z \rangle^2}$ is also shown, as well as the second moments $\langle S^z S^z \rangle$ and $\langle S^x S^x \rangle$, which approach the value $S(S+1)/3 = 2/3$ for large temperatures. For comparison the corresponding results of a MFT calculation are displayed in Figure 5b. For the same applied field the reorientation temperature $T_R \simeq 0.9\,T_C$ is considerably higher in this case. We emphasize the long tail in particular of the magnetization $M(T)$ at large temperatures in the RPA calculations of Figure 5a, which is absent in the MFT results of Figure 5b. This behaviour is due to the strong
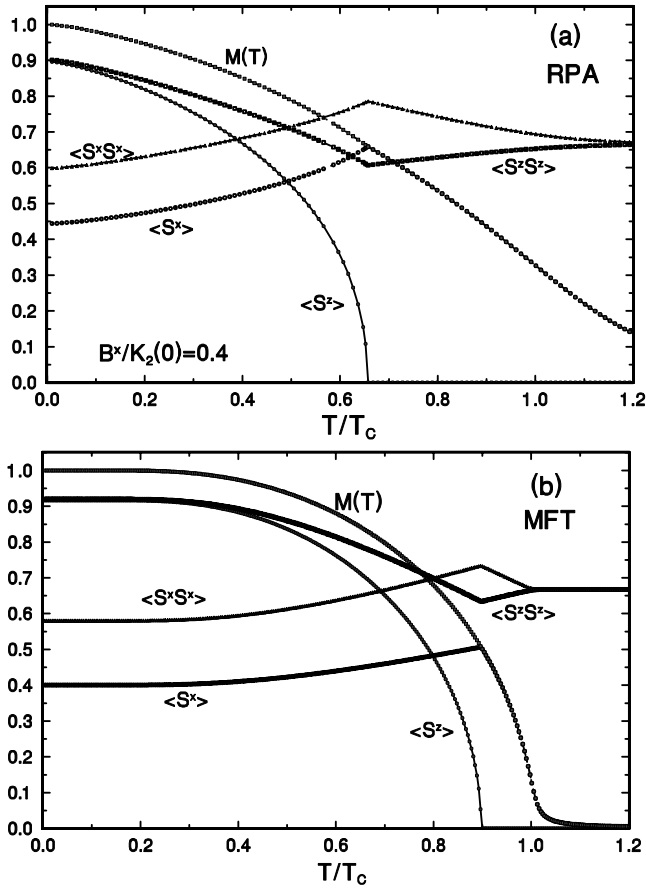
Fig. 6. Effective anisotropy coefficients $K_2(T)/K_2(0)$ calculated with RPA are displayed as functions of the reduced temperature T/T_C. The non-perturbative RPA result is compared with perturbative RPA results with external fields $B^z/K_2(0) = 0.01$, 0.1, and 1.

Fig. 5. Results of RPA (a) and MFT (b) calculations for the reorientation of the magnetization at a fixed magnetic field $B^x/K_2(0) = 0.4$ are shown as functions of the reduced temperature T/T_C. Displayed are the components $\langle S^z \rangle$ and $\langle S^x \rangle$ and the magnitude $M(T)$ of the magnetization, as well as the second moments $\langle S^z S^z \rangle$ and $\langle S^x S^x \rangle$.

effect of external magnetic fields on the properties of 2D Heisenberg magnets [10].

In reference [13] we showed the temperature dependence of the single-ion anisotropy coefficients of a ferromagnetic monolayer obtained with a thermodynamic perturbation theory. The magnetization was calculated in the framework of RPA, considering the isotropic exchange coupling and an external magnetic field B^z in the unperturbed Hamiltonian. In perturbation theory, it is unavoidable to apply a finite magnetic field in order to obtain a magnetization at finite temperatures (Mermin- Wagner theorem). Thus, the perturbative results for the effective anisotropy $K_2(T)$ depend sensitively on the strength of the magnetic field B^z. Even with this approach, we found significant differences from the corresponding mean-field theory calculations. As discussed in Section 2, equation (31) determines within RPA the effective single-ion anisotropy $K_2(T)$ non-perturbatively. In Figure 6 we compare the non-perturbative result for $K_2(T)$, already shown in Figure 4, with perturbative results as a function
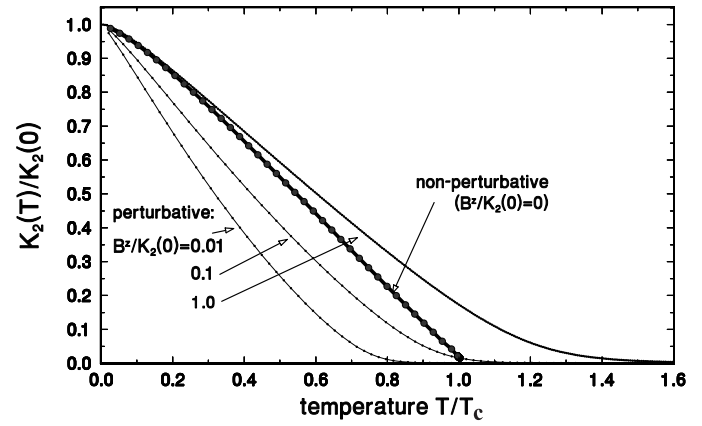
of the reduced temperature. We use $B^z/K_2(0) = 0.01$, 0.1, and 1.0. As already mentioned the absolute value of $K_2(T)/K_2(0)$ as calculated perturbatively depends considerably on the magnetic field B^z. Except for the rounding at elevated temperatures, which is clearly an effect of B^z, the shapes of $K_2(T)$ as calculated perturbatively and non-perturbatively within the RPA approach look similar to each other. The differences between perturbative and non-perturbative results become larger with increasing $K_2(0)$.

4 Discussion and conclusion

In the present paper, we have applied many-body Green's function theory for the calculation of the magnetic properties of a Heisenberg monolayer with second-order uniaxial single-ion anisotropy at finite temperatures. This method allows calculations over the entire temperature range of interest in contrast to other methods, which are only valid at low (Holstein-Primakoff approach) or high temperatures (high temperature expansions). We have used the Tyablikov (RPA) decoupling for the exchange interaction terms, and the Anderson-Callen decoupling for the anisotropy terms. For the latter, we have investigated various other decoupling schemes, which partly break down at higher temperatures or give results similar to the Anderson-Callen decoupling, see Appendix A. The results are far more sensitive to a variation of the strength of the anisotropy than to the different decoupling procedures. We emphasize the fact that the present method fulfills the Mermin-Wagner theorem in the limiting case of an isotropic 2D Heisenberg magnet, in contrast to the mean-field approximation applied formerly.

Our main investigations are concerned with the reorientation of the magnetization induced by a magnetic field perpendicular to the easy axis at finite temperatures, and

with a non-perturbative calculation of the temperature dependent (effective) anisotropy. We have in particular investigated the monolayer for spin $S = 1$ which is the lowest spin quantum number with a non-trivial second-order anisotropy. By solving the equations of motion for the Green's functions we calculate the components of the magnetization directly, which allows an immediate determination of the orientation angle. The effective anisotropy coefficient is calculated from the condition that the free energy has a minimum at the orientation angle. As discussed in Section 2 this is a non-perturbative approach in the sense that all quantities entering in the final expression are determined by the *full* Hamiltonian. This is shown to be an improvement over the usual thermodynamical perturbative treatment, where the unperturbed part of the Hamiltonian must contain the magnetic field. Therefore the corresponding results for the effective anisotropy necessarily depend on the magnetic field.

Prior to the present work, the magnetic reorientation and the effective anisotropies have been calculated mainly within the framework of mean-field theory (MFT) [6,7]. The magnetic reorientation has also been investigated with other theoretical methods [16,23]. In the presence of anisotropic interactions, MFT is expected to yield *qualitatively* correct results for 2D magnetic systems. By comparison, however, we find significant *quantitative* differences between the results obtained with MFT and the present Green's function theory. Owing to the magnetic fluctuations, one finds a different temperature scale with RPA as compared to MFT. With the same input parameters, the Curie temperature T_C of the present 2D system is about a factor of three larger in MFT than in RPA. If the temperature is rescaled with respect to the corresponding Curie temperatures the orientation angles of the magnetization look very similar in RPA and MFT. This we consider to be a non-trivial result because one would not expect this from the very beginning. The effective anisotropies, however, behave differently, also when rescaling the temperature. When using RPA the temperature dependence of the effective anisotropy coefficient behaves linearly over the whole temperature range $0 \leq T \leq T_C$. In MFT one observes an exponential dependence at low temperatures and small S. This different behaviour would manifest itself when extrapolating measurements performed at finite temperatures down to $T = 0$ in order to compare with *ab-initio* calculations [5] for the anisotropy coefficient $K_2(T = 0)$, which are available only there.

One also finds in RPA a stronger influence of the external magnetic field on the reorientation of the magnetization, which is reminiscent of 2D Heisenberg magnets [10]. We observe that, at a fixed temperature, a weaker reorientation field B_R^x is required in RPA than in MFT in order to align the magnetization along the field direction. At a fixed magnetic field, on the other hand, one obtains in RPA a lower reduced reorientation temperature T_R/T_C. Furthermore, the magnetization calculated by RPA has a long tail at large temperatures due to the magnetic field, which is absent in MFT results. In general, one expects the differences between RPA and MFT to decrease as the number of film layers increases.

Investigations into extending the model are in progress. The other decoupling procedure different from that of Anderson-Callen, which also works up to T_C, see Figure 7, will be investigated. In this case, none of the eigenvalues of the secular problem vanishes and one has to modify the formalism appropriately. A next step is to include the magnetic dipole coupling competing with the uniaxial single-ion anisotropy. The effect of the dipole coupling will become more important when the calculations are extended to magnetic films with several layers in order to treat also the dependence of the reorientation on the film thickness. In this case, the layer dependent anisotropies might lead to a temperature driven reorientation without the application of an external magnetic field, since the temperature dependence of the anisotropies will be different for surface and interior film layers. In addition, calculations for larger spins will be attempted, at least for spin $S = 2$, in order to be able to treat the fourth-order single-ion anisotropy K_4. Then one can set up a phase diagram *e.g.* in the $(K_2 - K_4)$-plane, which will show the region of stable magnetization directions and the location of the temperature driven magnetic reorientation. Furthermore, one can investigate whether the magnetic reorientation takes place continuously or discontinuously [6,7].

Appendix A: Decoupling schemes for the single-ion anisotropy term

In this appendix we discuss various decoupling procedures for the single-ion anisotropy term, and give arguments for using the Anderson-Callen decoupling. For an anisotropy *strong* compared to the exchange coupling, a method using different Green's functions has been applied formerly for spin $S = 1$ [24]. However, this method leads to an overdetermined system of equations for the expectation values $\langle S^z \rangle$ and $\langle S^z S^z \rangle$. On the other hand, for *small* anisotropies, as is the case for the magnetic systems considered in the present paper, different approaches have been proposed by Anderson-Callen [17] and by Lines [22], which we shall treat here.

For the decoupling of the higher-order Green's functions coming from the single-ion anisotropy term, an ansatz of the following form is used:

$$\langle\langle S_i^z S_i^\pm + S_i^\pm S_i^z; (S_j^z)^m (S_j^-)^n \rangle\rangle \simeq \Phi_i^{\pm,mn} G_{ij}^{\pm,mn} , \quad \text{(A.1)}$$

where the functions $\Phi_i^{\pm,mn}$ have to be determined. For $m = 0$, $n = 1$, Lines [22] proved that $\Phi_i^{+,01}$ can be expressed by the following ratios of commutators

$$\Phi_i^{+,01} = \frac{\langle [S_i^-, S_i^+(2S_i^z + 1)]\rangle}{\langle [S_i^-, S_i^+]\rangle} = \frac{3\langle (S_i^z)^2\rangle - S(S+1)}{\langle S_i^z\rangle} .$$
$$\text{(A.2)}$$

$$\tilde{\Phi}_i^{+,m1} = \frac{S(S+1)\langle (S_i^z)^m \rangle + (2S(S+1)-1)\langle (S_i^z)^{m+1} \rangle - 3\langle (S_i^z)^{m+2} \rangle - 2\langle (S_i^z)^{m+3} \rangle}{S(S+1)\langle (S_i^z)^m \rangle - \langle (S_i^z)^{m+1} \rangle - \langle (S_i^z)^{m+2} \rangle} \ . \tag{A.5}$$
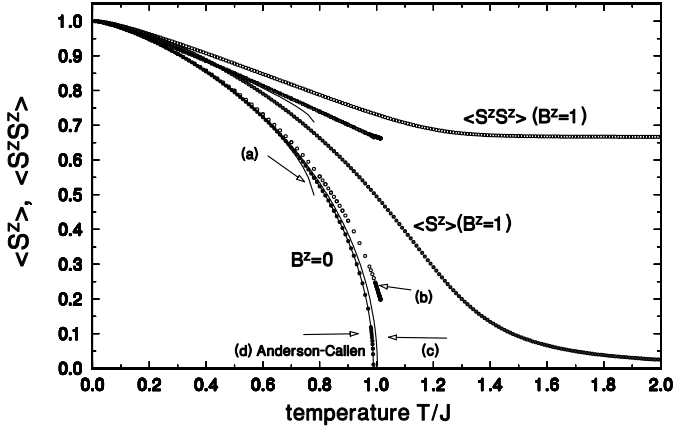

Fig. 7. The magnetization $\langle S^z \rangle$ and the second moment $\langle S^z S^z \rangle$ are shown as function of the temperature for various decoupling schemes discussed in the text. (a) Decoupling of equation (A.6); (b) decoupling of equation (A.7); (c) decoupling of equation (A.11); (d) Anderson-Callen decoupling (Eq. (A.13), small dots connected by thin line). Only the decouplings (c) and (d) work up to $\langle S^z \rangle = 0$, *i.e.*, up to the Curie temperature T_C, whereas (a) and (b) fail for $T < T_C$. We include also a result with Anderson-Callen decoupling and a magnetic field $B^z/K_2(0) = 1$.

For $m = n = 1$ one obtains

$$\Phi_i^{+,11} = \frac{\langle [S_i^z S_i^-, S_i^+ (2S_i^z + 1)] \rangle}{\langle [S_i^z S_i^-, S_i^+] \rangle}$$
$$= \frac{8\langle (S_i^z)^3 \rangle - 3\langle (S_i^z)^2 \rangle + (1 - 4S(S+1))\langle S_i^z \rangle + S(S+1)}{3\langle (S_i^z)^2 \rangle - \langle S_i^z \rangle - S(S+1)} \ . \tag{A.3}$$

Note that the $\Phi_i^{+,mn}$ depend only on a single lattice site i, as expected. Similar expressions may be derived for $\Phi_i^{-,mn}$.

An alternative expression for $\Phi_i^{+,mn}$ can be obtained by replacing the Green's functions in equation (A.1) by their respective expectation values, resulting in

$$\langle (S_i^z)^m (S_i^-)^n (S_i^z S_i^\pm + S_i^\pm S_i^z) \rangle$$
$$\simeq \tilde{\Phi}_i^{\pm,mn} \langle (S_i^z)^m (S_i^-)^n S_i^\pm \rangle . \tag{A.4}$$

One obtains for $n = 1$

$$\text{see equation (A.5) above}$$

For spin $S = 1$, which we treat in the present paper, we need $m = 0, 1$ and $n = 1$. One has $S(S+1) = 2$, $(S_i^z)^3 = S_i^z$, and $(S_i^z)^4 = (S_i^z)^2$, thus the ratios of commutators are

$$\Phi_i^{+,01} = \frac{3\langle (S_i^z)^2 \rangle - 2}{\langle S_i^z \rangle} \ , \qquad \Phi_i^{+,11} = -1, \tag{A.6}$$

and the ratios of the expectation values are given by

$$\tilde{\Phi}_i^{+,01} = \frac{2 + \langle S_i^z \rangle - 3\langle (S_i^z)^2 \rangle}{2 - \langle S_i^z \rangle - \langle (S_i^z)^2 \rangle} \ , \qquad \tilde{\Phi}_i^{+,11} = -1 . \tag{A.7}$$

Note that Lines [22] mixes both approaches, since he uses equation (A.2) for even m and equation (A.5) for odd m.

In order to investigate the differences between these decoupling procedures, we treat the special case $B^x = B^y = 0$, for which $\langle S_i^x \rangle = \langle S_i^y \rangle = 0$. Then one has to determine the expectation values $\langle S_i^z \rangle$ and $\langle S_i^z S_i^z \rangle$. For $S = 1$ we obtain from equations (32) and (33), dropping the site index i for the ferromagnetic system,

$$\langle (S^z)^2 \rangle = 2 - \langle S^z \rangle (1 + 2\phi_0)$$
$$\langle S^z \rangle = \frac{1 + 2\phi_0}{1 + 2\phi_1 + \phi_0 + 3\phi_1\phi_0} \ , \tag{A.8}$$

with

$$\phi_m = \frac{1}{N} \sum_{\mathbf{k}} \left(\exp(\beta E_{\mathbf{k}}^m) - 1 \right)^{-1} \tag{A.9}$$

$$E_{\mathbf{k}}^m = B^z + \langle S^z \rangle J(4 - \gamma_{\mathbf{k}}) + K_2 \Phi^m \ , \tag{A.10}$$

with $m = 0, 1$, where Φ^m is either $\Phi^{+,m1}$ or $\tilde{\Phi}^{+,m1}$.

When solving these equations for the decoupling procedures (A.6, A.7), we find that both procedures fail at temperatures far below T_C, (*cf.* Fig. 7 (situation (a),(b)). Thus one cannot use both decouplings up to the Curie temperature T_C. When calculating Curie temperatures, Lines [22] has circumvented the problem associated with equations (A.8) by (inconsistently) using in the *dispersion relations* $E_{\mathbf{k}}^m$, equation (A.10), expectation values $\langle S^z \rangle$ and $\langle S^z S^z \rangle$ as obtained from the one-particle density operator, using a theorem originating from Callen and Strikman [25].

If, however, one uses

$$\Phi^{+,m1} = \Phi^{+,01} \ (\text{or } \tilde{\Phi}^{+,m1} = \tilde{\Phi}^{+,01}, \text{respectively}) \tag{A.11}$$

for $m = 0, 1$, the procedure works well and yields reasonably results for $\langle S^z \rangle$ and $\langle S^z S^z \rangle$ between $T = 0$ and $T = T_C$, *cf.* Figure 7c, and the following discussion about the Curie temperature T_C. In this case, $\phi_0 = \phi_1 \equiv \phi$, see equation (A.9), and one finds that the procedures for $\Phi^{+,01}$ and $\tilde{\Phi}^{+,01}$ give the same result. This can be understood by equating $\Phi^{+,01} = \tilde{\Phi}^{+,01}$, which yields the second of equations (A.8) determining $\langle S^z \rangle$.

Using this decoupling in the Green's function formalism one can derive expressions for the $\Phi^{-,mn}$, using also $\Phi^{-,01} = \Phi^{-,11}$. This leads to a 3×3 secular problem for equation (6) with three non-vanishing eigenvalues, since here $\Phi^{+,mn} \neq \Phi^{-,mn}$. In this case the regularity condition (20) cannot be applied. This case is more complicated to

handle than the Anderson-Callen decoupling, in which one of the eigenvalues vanishes, *cf.* equation (13).

The Anderson-Callen decoupling is based on the paper by Callen [26], in which correlations beyond the RPA are included in the decoupling of the Green's functions of the *exchange* terms. In this case, the essential Green's function is non-diagonal ($i \neq j$) and the decoupling reads (*e.g.* for $m = 0$, $n = 1$)

$$\langle\langle S_i^z S_j^\pm; S_k^- \rangle\rangle \simeq \langle S_i^z \rangle \langle\langle S_j^\pm; S_k^- \rangle\rangle$$
$$- \frac{\langle S_i^z \rangle}{2S^2} \langle S_i^\mp S_j^\pm \rangle \langle\langle S_i^\pm; S_k^- \rangle\rangle. \quad (A.12)$$

Neglecting the second term corresponds to the RPA decoupling.

The proposal of Anderson and Callen [17] is to use the same decoupling also for Green's functions with $i = j$, resulting from the anisotropy terms

$$\langle\langle (S_i^z S_i^\pm + S_i^\pm S_i^z); S_k^- \rangle\rangle$$
$$\simeq 2\langle S_i^z \rangle \left\{ 1 - \frac{1}{4S^2} \left[\langle S_i^\mp S_i^\pm \rangle + \langle S_i^\pm S_i^\mp \rangle \right] \right\} \langle\langle S_i^\pm; S_k^- \rangle\rangle$$
$$= 2\langle S_i^z \rangle \left\{ 1 - \frac{1}{2S^2} \left[\langle S(S+1) - \langle S_i^z S_i^z \rangle \rangle \right] \right\} \langle\langle S_i^\pm; S_k^- \rangle\rangle$$
$$= \Phi^\pm \langle\langle S_i^\pm; S_k^- \rangle\rangle. \quad (A.13)$$

In this case, one does not distinguish between different m. Since here $\Phi^+ = \Phi^- = \Phi$, which is the quantity Φ given in equation (9), one of the eigenvalues turns out to be zero, *cf.* equation (13). This is a prerequisite for being able to use the procedure outlined in Section 2 for the determination of the expectation values $\langle S^z \rangle$ and $\langle S^z S^z \rangle$.

Inspecting Figure 7 shows that the two decouplings, which work up to the Curie temperature, do not give very different results. Therefore, we adopt the decoupling which is easier to apply: the Anderson-Callen decoupling.

In the remainder of this appendix, we derive expressions which determine the Curie temperature, $T_C(J, K_2)$, for the case $S = 1$ and $\Phi^{+,01} = \Phi^{+,11} = \Phi$, *cf.* equation (A.11). The consideration of different $\Phi^{+,01} \neq \Phi^{+,11}$, *cf.* equation (A.6), leads to severe complications whilst determining T_C, or, as we have seen, when calculating the magnetization $\langle S^z \rangle$ as function of T.

T_C is calculated from performing the limit $\langle S^z \rangle \to 0$ in equations (A.8). To lowest order in $\langle S^z \rangle$, one obtains for $T \to T_C$

$$\langle (S^z)^2 \rangle (T \lesssim T_C) \approx 2/3 + \langle S^z \rangle^2/4, \quad (A.14)$$

and for the decoupling functions

$$\Phi(T_C) = \alpha \langle S^z \rangle, \quad (A.15)$$

with $\alpha = 3/4$ for the decoupling given by equation (A.11) and $\alpha = 2/3$ for the Anderson-Callen decoupling, equations (9) or (A.13). Close to T_C one also obtains from equation (A.9)

$$\phi(T_C) \approx \frac{T_C}{\langle S^z \rangle} \frac{1}{N} \sum_{\mathbf{k}} \left(J(4 - 2\gamma_{\mathbf{k}}) + K_2 \alpha \right)^{-1}, \quad (A.16)$$
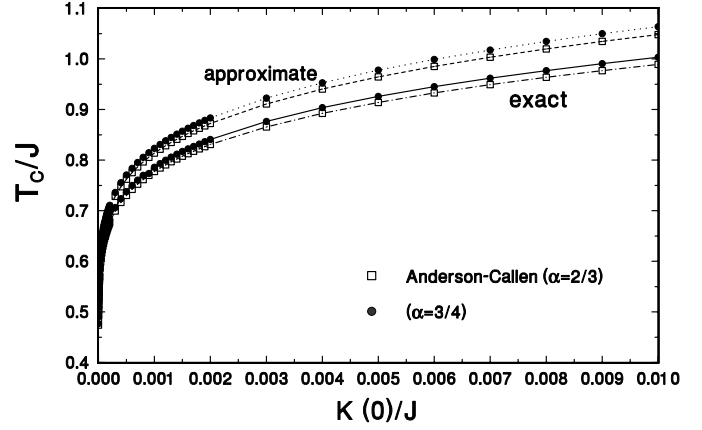

Fig. 8. Curie temperatures normalized to the exchange coupling, T_C/J; are shown as a function of the anisotropy strength $K_2(0)/J$, using equation (A.15) with $\alpha = 3/4$ (decoupling according to Equation (A.11)) and $\alpha = 2/3$ corresponding to the Anderson-Callen decoupling (Eq. (A.13). The Curie temperatures at $K_2(0)/J = 0.01$ correspond to those of Figure 7 (cases (c) and (d)). Also, the results from the approximate expression, equation (A.19), for $\alpha = 3/4$ and $\alpha = 2/3$ are included in the figure.

and from equation (A.8)

$$\phi(T_C) \approx \frac{2}{3\langle S^z \rangle}. \quad (A.17)$$

Combining these equations and converting the sum into an integral gives

$$T_C = \frac{8\pi^2}{3} \left(\int_{-\pi}^{\pi} dk_x \int_{-\pi}^{\pi} dk_y \frac{1}{J(4 - \gamma_{\mathbf{k}}) + K_2 \alpha} \right)^{-1}. \quad (A.18)$$

The Curie temperatures calculated with this formula are displayed in Figure 8 for the two single-ion decouplings under consideration.

Since this integral is dominated by small wave numbers it can be approximately evaluated when expanding $\gamma_{\mathbf{k}}$ up to the leading order in $\mathbf{k}$:

$$T_C = \frac{8\pi J/3}{\ln(1 + 2\pi^2 J/K_2 \alpha)} . \quad (A.19)$$

This expression can be used as a quick estimate for the Curie temperature. It overestimates the result as obtained from equation (A.18) by less than 10%. The corresponding results are also shown in Figure 8.

We emphasize the fact that the various decoupling procedures do not yield very different results for the magnetization, see Figure 7, or the Curie temperature T_C, *cf.* Figure 8. We note that the results are much more sensitive to varying the strength of the anisotropy coefficient $K_2(0)$ than to the different decoupling procedures. This is shown in Figure 9 by plotting the magnetization $\langle S^z \rangle$ and $\langle S^z S^z \rangle$ as function of the temperature for different values $K_2(0)/J$ of the anisotropy coefficient normalized to the exchange coupling strength J for the case of the Anderson-Callen decoupling.

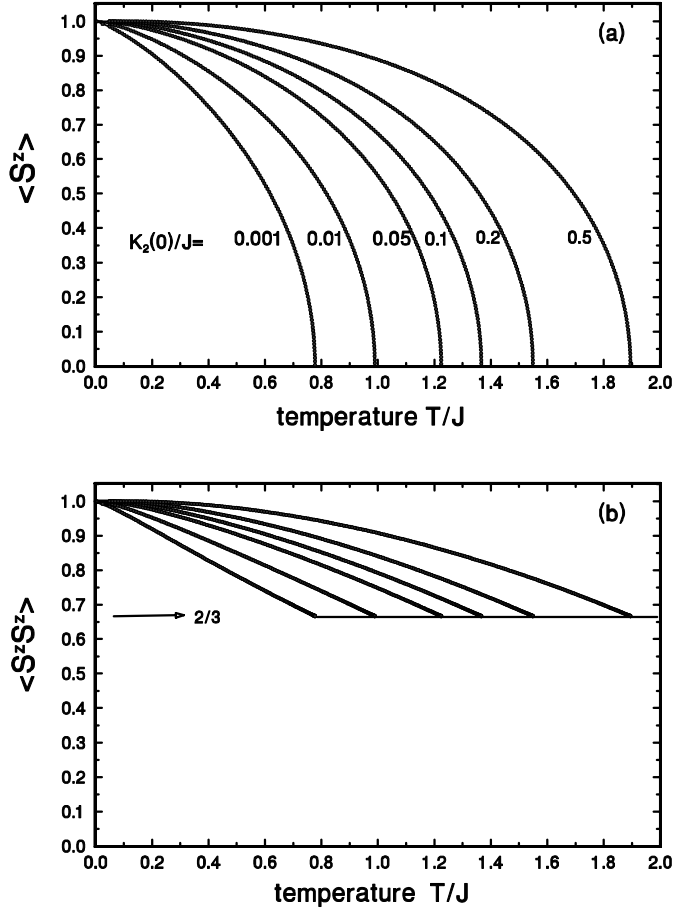| m	n	$A_{-1}^{z,mn}$	$A_{-1}^{+,mn}$	$A_{-1}^{-,mn}$
0	1	$-\langle S^-\rangle$	$2\langle S^z\rangle$	0
0	2	$-2\langle S^-S^-\rangle$	$4\langle S^zS^-\rangle + 2\langle S^-\rangle$	0
1	1	$-\langle S^zS^-\rangle$	$3\langle S^zS^z\rangle - \langle S^z\rangle - S(S+1)$	$\langle S^-S^-\rangle$
0	3	$-3\langle S^-S^-S^-\rangle$	$6\langle S^zS^-S^-\rangle + 6\langle S^-S^-\rangle$	0
1	2	$-2\langle S^zS^-S^-\rangle$	$5\langle S^zS^zS^-\rangle + \langle S^zS^-\rangle - \langle S^-\rangle S(S+1)$	$\langle S^-S^-S^-\rangle$
2	1	$-\langle S^zS^zS^-\rangle$	$4\langle S^zS^zS^z\rangle - 3\langle S^zS^z\rangle$ $+(1 - 2S(S+1))\langle S^z\rangle + S(S+1)$	$2\langle S^zS^-S^-\rangle + \langle S^-S^-\rangle$

Fig. 9. The temperature dependence of $\langle S^z\rangle$ (a) and $\langle S^zS^z\rangle$ (b) for different strengths of the anisotropy coefficient $K_2(0)/J = 0.001$, 0.01, 0.05, 0.01, 0.2, and 0.5 is displayed.

Appendix B

In this Appendix we list explicitly a number of relations obtained from the regularity condition equation (19)

$$-2ZA_{-1}^{z,mn} = A_{-1}^{+,mn}B^- + A_{-1}^{-,mn}B^+. \tag{B.1}$$

Remember that we have used the notations $B^\pm = B^x \pm i\,B^y$, $Z = B^z + K_2\,\Phi$, and $A_{-1}^{\alpha,mn} = \langle[S^\alpha,(S^z)^m(S^-)^n]_{-1}\rangle$. First we tabulate some commutator relations

see Tab. above

Then we obtain with $m = 0, n = 1$

$$\langle S^\pm\rangle = \frac{B^\pm}{Z}\langle S^z\rangle, \tag{B.2}$$

with $m = 0, n = 2$ and $m = 1, n = 1$

$$\langle S^-S^-\rangle = \frac{(B^-)^2}{2Z^2 - B^+B^-}\Big(3\langle S^zS^z\rangle - S(S+1)\Big)$$

$$\langle S^zS^-\rangle = \frac{B^-Z}{2Z^2 - B^+B^-}\Big(3\langle S^zS^z\rangle - S(S+1)\Big) - \frac{B^-}{2Z}\langle S^z\rangle, \tag{B.3}$$

and with $m = 0, n = 3$, and $m = 1$, $n = 2$, and $m = 2$, $n = 1$

$$\langle S^zS^zS^-\rangle =$$
$$\frac{B^-Z}{2Z^2 - 3B^+B^-}\Big[4\langle S^zS^zS^z\rangle - \langle S^z\rangle\Big(2S(S+1) - 1\Big)$$
$$- \Big(3\langle S^zS^z\rangle - S(S+1)\Big)\frac{2Z^2 - 3B^+B^-}{2Z^2 - B^+B^-}$$
$$- \frac{B^+B^-}{Z^2}\Big(\langle S^zS^zS^z\rangle + \frac{1}{2}\langle S^z\rangle\Big)\Big]$$
$$\langle S^zS^-S^-\rangle =$$
$$\frac{(B^-)^2}{2Z^2 - 3B^+B^-}\Big[5\langle S^zS^zS^z\rangle - \langle S^z\rangle\Big(3S(S+1) - 1\Big)$$
$$- \Big(3\langle S^zS^z\rangle - S(S+1)\Big)\frac{2Z^2 - 3B^+B^-}{2Z^2 - B^+B^-}\Big]$$
$$\langle S^-S^-S^-\rangle =$$
$$\frac{(B^-)^3}{Z(2Z^2 - 3B^+B^-)}\Big[5\langle S^zS^zS^z\rangle - \langle S^z\rangle\Big(3S(S+1) - 1\Big)\Big]. \tag{B.4}$$

References

1. J.A.C. Bland, B. Heinrich, in *Ultrathin Magnetic Structures* (Springer Verlag, Berlin, 1994).
2. G. Lugert, W. Robl, L. Pfau, M. Brockmann, G. Bayreuther, J. Magn. Magn. Mater. **121**, 498 (1993); O. Schulte, F. Klose, W. Felsch, Phys. Rev. B **52**, 6480 (1995); M. Farle, B. Mirwald-Schulz, A.N. Anisimov, W. Platow, K. Baberschke, Phys. Rev. B **55**, 3708 (1997), and references therein.
3. J.R. Dutcher, J.F. Cochran, I. Jacob, W.F. Egelhoff, Jr., Phys. Rev. B **39**, 10430 (1989).

4. Y.T. Millev, H.P. Oepen, J. Kirschner, Phys. Rev. B **57**, 5837, 5848 (1998); A. Hucht and K.D. Usadel, preprint `cond-mat/9903040`.

5. O. Hjortstam, K. Baberschke, J.M. Wills, B. Johansson, O. Erickson, Phys. Rev. B **55**, 15026 (1997); C. Uiberacker, J. Zabloudil, P. Weinberger, L. Szunyogh, C. Sommers, Phys. Rev. Lett. **82**, 1289 (1999), and references therein.

6. A. Moschel, K.D. Usadel, Phys. Rev. B **49**, 12868 (1994); P.J. Jensen, K.H. Bennemann, in *Magnetism and Electronic Correlations in Local-Moment Systems: Rare-Earth Elements and Compounds*, edited by M. Donath, P.A. Dowben, W. Nolting (World Scientific, Singapore, 1998), pp. 113-141.

7. P.J. Jensen, K.H. Bennemann, Solid State Comm. **100**, 585 (1996); *ibid.* **105**, 577 (1998); A. Hucht, K.D. Usadel, Phys. Rev. B **55**, 12309 (1997).

8. N.M. Mermin, H. Wagner, Phys. Rev. Lett. **17**, 1133 (1966).

9. C. Herring, C. Kittel, Phys. Rev. **81**, 869 (1951); S.V. Maleev, Sov. Phys. JETP **43**, 1240 (1976); V.L. Pokrovsky, M.V. Feigel'man, *ibid.,* **45**, 291 (1977).

10. D.A. Yablonsky, Phys. Rev. B **44**, 4467 (1991); D. Kerkmann, D. Pescia, R. Allenspach, Phys. Rev. Lett. **68**, 686 (1992).

11. R.P. Erickson, D.L. Mills, Phys. Rev. B **43**, 10715 (1991); *ibid.* **44**, 11825 (1991).

12. T. Holstein, H. Primakoff, Phys. Rev. **58**, 1098 (1940).

13. A. Ecker, P. Fröbrich, P.J. Jensen, P.J. Kuntz, J. Phys. Cond. Matter **11**, 1557 (1999).

14. S.V. Tyablikov, in *Methods in the quantum theory of magnetism* (Plenum Press, New York, 1967); K. Elk, W. Gasser, in *Die Methode der Greenschen Funktionen in der Festkörperphysik* (Akademie-Verlag, Berlin, 1978); W. Nolting, in *Quantentheorie des Magnetismus,* vol. 2 (B.G. Teubner, Stuttgart, 1986).

15. C. Timm, S.M. Girvin, P. Henelius, A.W. Sandvik, Phys. Rev. B **58**, 1464 (1998).

16. M.M. Taylor, B.L. Györffy, J. Phys. Cond. Matter **5**, 4527 (1993); A. Moschel, K.D. Usadel, Phys. Rev. B **51**, 16111 (1995); A. Hucht, A. Moschel, K.D. Usadel, J. Magn. Magn. Mater. **148**, 32 (1995).

17. F.B. Anderson, H.B. Callen, Phys. Rev. **136**, A1068 (1964).

18. Y. Millev, M. Fähnle, Phys. Rev. B **32**, 4336 (1995).

19. T.H. Moos, W. Hübner, K.H. Bennemann, Solid State Commun. **98**, 639 (1996).

20. S.V. Tyablikov, Ukr. Mat. Zh. **11**, 287 (1959).

21. A. Narath, Phys. Rev. **140**, A854 (1965).

22. M.E. Lines, Phys. Rev. **156**, 534 (1967).

23. P. Politi, A. Rettori, M.G. Pini, D. Pescia, J. Magn. Magn. Mater. **140-144**, 647 (1995); X. Hu, Y. Kawazoe, Phys. Rev. B **54**, 65 (1996); T. Herrmann, M. Potthoff, W. Nolting, Phys. Rev. B **58**, 831 (1998).

24. T. Egami, M.S.S. Brooks, Phys. Rev. B **12**, 1021, 1029 (1975); S.B. Haley, *ibid.,* **17**, 337 (1978).

25. H.B. Callen, S. Strickman, Solid State Commun. **3**, 5 (1965).

26. H.B. Callen, Phys. Rev. **130**, 890 (1963).